On the design and implementation of linear differential microphone arrays

Jingdong Chen, Jacob Benesty, and Chao Pan

Citation: The Journal of the Acoustical Society of America **136**, 3097 (2014); doi: 10.1121/1.4898429
View online: https://doi.org/10.1121/1.4898429
View Table of Contents: https://asa.scitation.org/toc/jas/136/6
Published by the Acoustical Society of America

On the design and implementation of linear differential microphone arrays

Jingdong Chen[a)]
Center of Intelligent Acoustics and Immersive Communications, Northwestern Polytechnical University, 127 Youyi West Road, Xi'an, Shaanxi 710072, China

Jacob Benesty
INRS-EMT, University of Quebec, 800 de la Gauchetiere Ouest, Suite 6900, Montreal, Quebec H5A 1K6, Canada

Chao Pan
Northwestern Polytechnical University, 127 Youyi West Road, Xi'an, Shaanxi 710072, China

(Received 14 February 2014; revised 28 August 2014; accepted 7 October 2014)

Differential microphone array (DMA), a particular kind of sensor array that is responsive to the differential sound pressure field, has a broad range of applications in sound recording, noise reduction, signal separation, dereverberation, etc. Traditionally, an Nth-order DMA is formed by combining, in a linear manner, the outputs of a number of DMAs up to (including) the order of $N-1$. This method, though simple and easy to implement, suffers from a number of drawbacks and practical limitations. This paper presents an approach to the design of linear DMAs. The proposed technique first transforms the microphone array signals into the short-time Fourier transform (STFT) domain and then converts the DMA beamforming design to simple linear systems to solve. It is shown that this approach is much more flexible as compared to the traditional methods in the design of different directivity patterns. Methods are also presented to deal with the white noise amplification problem that is considered to be the biggest hurdle for DMAs, particularly higher-order implementations.
 [http://dx.doi.org/10.1121/1.4898429]

PACS number(s): 43.60.Fg, 43.72.Dv [TFD] Pages: 3097–3113

I. INTRODUCTION

Microphone array is a generic expression used to refer to a sound system that has multiple microphones. These microphones can be either distributed into an arbitrary network (often called a sensor network) or arranged into a particular geometry (called an organized array) (Huang *et al.*, 2011). In most of the cases, however, when we say microphone arrays, we mean organized arrays in which the sensors' positions relative to a reference point are known to the subsequent processors. These kind of arrays can be used to solve many important problems such as source localization/tracking, noise reduction/speech enhancement, source separation, dereverberation, spatial sound recording, etc., and, consequently, the design of such microphone arrays and the associated processing algorithms has attracted a significant amount of research and engineering interest over the last four decades. Many different array systems have been developed, which can be categorized into two basic classes depending on how they respond to the sound field, i.e., additive and differential arrays.

Additive microphone arrays achieve signal enhancement and noise reduction via the synchronize-and-add principle, but they have now evolved to include all the arrays with large inter-element spacing (from a couple of centimeters to a couple of decimeters) and optimal beamforming in broadside directions. This kind of arrays have been proven to be useful in dealing with many problems (Brandstein and Ward, 2001; Huang *et al.*, 2006; Benesty *et al.*, 2008). However, they are also found to suffer from a number of limitations in processing broadband signals such as speech. First, the beampattern of an additive array is frequency dependent and the beamwidth is inversely proportional to the frequency. As a result, such an array is not effective in dealing with low-frequency noise and interference. Second, since the beamwidth is larger at low frequencies than at high frequencies, directional noise and interference are attenuated in a non-uniform way (more attenuation at high frequencies and less attenuation at low frequencies) over its entire frequency spectrum, leading to some disturbing artifacts at the array's output (Ward *et al.*, 1998). Furthermore, if the incident angle of the desired speech source is different from the array's look direction, which happens often in practice, the speech signal will be low-pass filtered, leading to speech spectral distortion.

To overcome those aforementioned drawbacks, the so-called broadband beamforming techniques have been studied. One way to obtain a broadband beamformer is to use harmonically nested subarrays (Flanagan *et al.*, 1985; Flanagan *et al.*, 1991; Kellermann, 1991; Elko and Meyer, 2008). In every subarray, the sensors are equally spaced, and the subarray is designed for operating at a single frequency. By using a different sensor spacing and different number of microphones with subarrays, the nested array can be controlled to have a similar spatial response across the frequency range of interest. But such a solution usually requires

[a)]Author to whom correspondence should be addressed. Electronic mail: jingdongchen@ieee.org

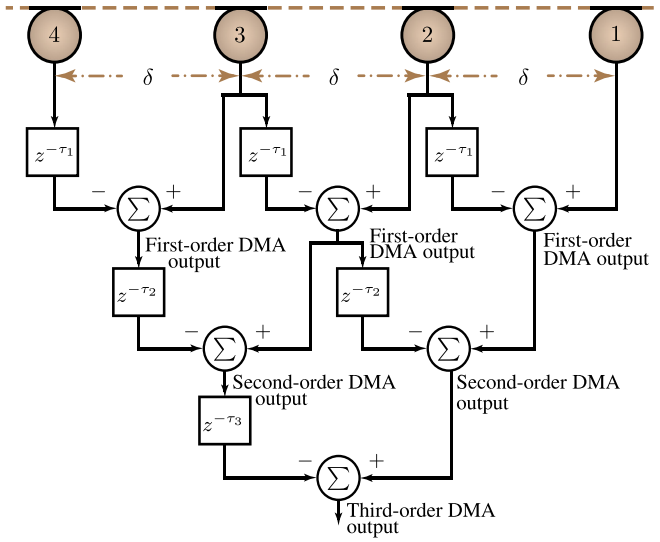

FIG. 1. (Color online) Traditional implementation of first-, second-, and third-order DMAs, where δ is the inter-element spacing and the delay parameters τ_1, τ_2, and τ_3 are used to control the null positions.

a large array with a large number of microphones even though subarrays may share sensors in the array. Another more economic way to design a broadband beamformer is through narrowband decomposition. A narrowband beamformer is then designed in each subband with a constraint applied to control the beamwidth so that all the beamformers from different subbands have the same beamwidth. Though it can make constant beamwidth across a wide range of frequencies, this approach to broadband beamforming sacrifices the array performance in high frequencies. This subband approach can also be implemented using the filter-and-sum framework, i.e., applying a finite impulse response (FIR) filter to every sensor signal and then sums up all the filtered signals to form the array's output (Frost, 1972). Constant beamwidth can be achieved with this framework by properly adjusting the coefficients of those FIR filters. However, the array spatial response of such broadband beamformers are still frequency-varying regardless of the structure.

Differential microphone arrays (DMAs) are responsive to the spatial derivatives of the acoustic pressure field. In comparison with additive arrays, DMAs can have many advantages in processing broadband signals. First, a DMA can form frequency-invariant beampatterns as it will be discussed later. This makes it effective for processing both low- and high-frequency signals. Second, a DMA has the potential to attain maximum directional gain with a given number of sensors (Elko, 2000; Elko and Meyer, 2008). Furthermore, DMAs are generally small in size (relative to the acoustic wavelength) due to the inherent assumption that the true pressure differentials can be approximated by finite differences of microphone outputs. Therefore, DMAs can be easily integrated into communication devices. As a consequence, the design of DMAs and the associated beamforming algorithms have attracted much interest over the past few decades.

Traditionally, an Nth-order DMA is formed by using $N+1$ microphones and its output is generated by subtractively combining the outputs of two DMAs of order $N-1$, as illustrated in Fig. 1 (Elko and Meyer, 2008; Elko, 2000; Sessler and West, 1971; Olson, 1946; Elko *et al.*, 2003; Abhayapala and Gupta, 2010; Kolundžija *et al.*, 2011). This way of DMA design, though simple and easy to implement, has many drawbacks. The most prominent problems are (1) it lacks flexibility in forming different beampattens; and (2) it is difficult to deal with the problem of white noise amplification, particularly at low frequencies.

Recently, we developed an approach to the design and implementation of uniform linear DMAs (Benesty and Chen, 2013). The basic idea is illustrated in Fig. 2, which adopted the widely used analysis-and-synthesis framework in speech processing (Lim, 1979; Benesty *et al.*, 2009). First, the signals received by the DMA is partitioned into small overlapping frames. Every frame is then transformed into the short-time Fourier transform (STFT) domain. In every STFT subband, a differential beamformer is designed and applied to

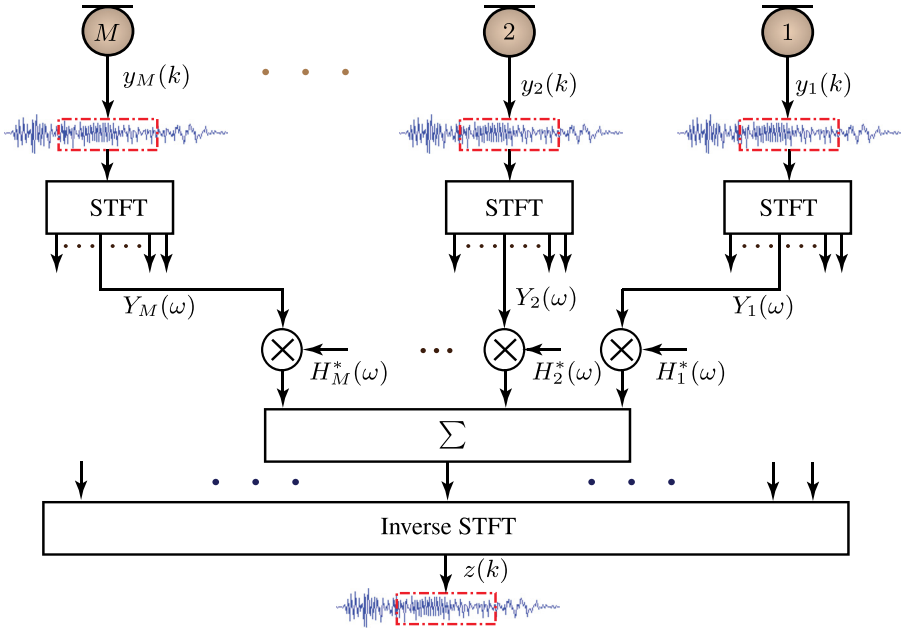

FIG. 2. (Color online) Illustration of the DMA design approach in the STFT domain.

the multichannel STFT coefficients to reduce noise and estimate the desired signal in the corresponding subband. Finally, the time-domain signal estimate is constructed using either the overlap-add or overlap-save technique with the inverse STFT. The most crucial step in this framework is the design of the differential beamformers in the STFT subbands, which was preliminarily studied in Benesty and Chen (2013). This paper is an extension of the work presented in Benesty and Chen (2013). The major contributions of this paper are threefold: (1) the DMA design approach is presented in a more systematic and rigorous way; (2) we cover some of the important design cases (including beampatterns with distinct nulls and nulls of multiplicity of more than one) that were not discussed in Benesty and Chen (2013); and, most importantly, (3) we present two methods to deal with the white noise amplification problem, which is a major issue in DMA design.

The remainder of this paper is organized as follows. In Sec. II, we present the signal model and the problem of beamforming. We then give three important performance measures (beampattern, white noise gain, and directivity index) in Sec. III, which are widely used for the evaluation of beamformers. In Sec. IV, we discuss the ideal beampatterns of DMAs with different orders. In Sec. V, we describe a general approach to the design of an Nth-order DMA using $N+1$ microphones. Then, in Sec. VI, we present two robust approaches that use more than $N+1$ microphones to design an Nth-order DMA and can deal with the white noise amplification problem. In Sec. VII, we briefly discuss a possible design of an Nth-order DMA with less than $N+1$ microphones. Finally, a summary is given in Sec. VIII.

II. SIGNAL MODEL AND PROBLEM FORMULATION

Let us consider a uniform linear array consisting of M omnidirectional microphones as illustrated in Fig. 3, where the inter-element spacing is equal to δ. Suppose that there is a planewave, propagating in an anechoic environment at the speed of sound, i.e., $c = 340$ m/s, and impinging on the array with an incident angle of θ. In this scenario, the signal received at the mth ($m = 1, 2, \ldots, M$) microphone, at the discrete-time index k, is given by

$$y_m(k) = x[k - (m-1)\tau_0 \cos\theta] + v_m(k), \tag{1}$$

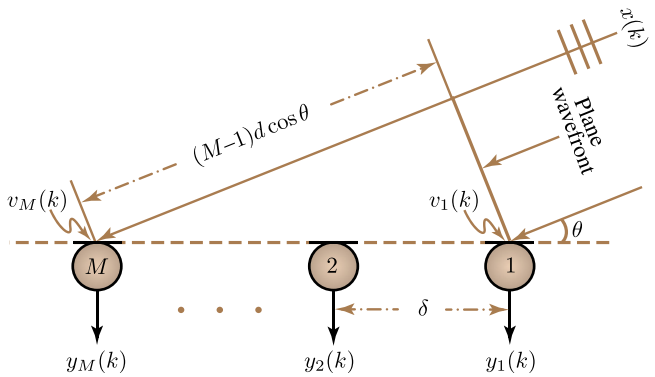

FIG. 3. (Color online) Illustration of a uniform linear microphone array system.

where $x(k)$ is the signal of interest, $v_m(k)$ is the noise observed at the mth microphone, $\tau_0 = \delta/c$ is the delay between the first two sensors (the first sensor is chosen as the reference) at the angle $\theta = 0°$.

If we follow the paradigm shown in Fig. 2 and transform the signals in (1) into the STFT domain, we get

$$Y_m(\omega) = e^{-j(m-1)\omega\tau_0 \cos\theta} X(\omega) + V_m(\omega), \tag{2}$$

where $X(\omega)$, $V_m(\omega)$, and $Y_m(\omega)$ are the STFT of $x(k)$, $v_m(k)$, and $y_m(k)$, respectively (note that we neglect the frame index for ease of exposition), j is the imaginary unit with $j = \sqrt{-1}$, and $\omega = 2\pi f$ is the angular frequency.

In a vector form, (2) can be rewritten as

$$\begin{aligned}\mathbf{y}(\omega) &\triangleq [Y_1(\omega)\, Y_2(\omega) \cdots Y_M(\omega)]^T \\ &= \mathbf{d}(\omega, \cos\theta) X(\omega) + \mathbf{v}(\omega),\end{aligned} \tag{3}$$

where the noise signal vector, $\mathbf{v}(\omega)$, is defined similarly to $\mathbf{y}(\omega)$,

$$\mathbf{d}(\omega, \cos\theta) \triangleq [1 \;\; e^{-j\omega\delta\cos\theta/c} \cdots e^{-j(M-1)\omega\delta\cos\theta/c}]^T \tag{4}$$

is a phase-delay vector of length M (which is the same as the steering vector used in traditional beamforming) and the superscript T is the transpose operator.

The objective of this paper is to design DMA beamformers that can recover the signal of interest, $X(\omega)$, given $\mathbf{y}(\omega)$. For that, a complex weight, $H_m^*(\omega)$, is applied to the output of the mth microphone, $m = 1, 2, \ldots, M$, where the superscript * denotes complex conjugation. The weighted outputs are then summed together to form the beamformer output as shown in Fig. 2. Putting all the weights together to form a vector of length M, we get

$$\mathbf{h}(\omega) = [H_1(\omega)\, H_2(\omega) \cdots H_M(\omega)]^T. \tag{5}$$

The beamformer output is then

$$\begin{aligned}Z(\omega) &= \sum_{m=1}^{M} H_m^*(\omega) Y_m(\omega) = \mathbf{h}^H(\omega)\mathbf{y}(\omega) \\ &= \mathbf{h}^H(\omega)\mathbf{d}(\omega, \cos\theta) X(\omega) + \mathbf{h}^H(\omega)\mathbf{v}(\omega),\end{aligned} \tag{6}$$

where $Z(\omega)$ is an estimate of the signal of interest, $X(\omega)$, and the superscript H is the conjugate-transpose operator. The problem of beamforming is then to find $\mathbf{h}(\omega)$ so that $Z(\omega)$ is a good estimate of $X(\omega)$. As pointed out in the previous section, there are two different types of arrays, resulting in two different approaches to beamforming: additive and differential. The former deals with arrays with large apertures while the latter handles arrays with small apertures (as compared to the wavelength). The focus of this paper is on differential beamforming with small apertures, which is to design beamformers whose beampatterns are good approximations of the "ideal" DMA patterns (Buck, 2002).

In order for the beampatterns to be close to the ideal DMA patterns or, in other words, for the array to be responsive to the differential sound field, we need to make the following assumptions.

(1) We assume that the sensor spacing, δ, is much smaller than the acoustic wavelength, $\lambda = c/f$, i.e., $\delta \ll \lambda$ (this implies that $\omega\tau_0 \ll 2\pi$). This assumption is required so that the true acoustic pressure differentials can be approximated by finite differences of the microphones' outputs.
(2) In linear DMAs, the mainlobe of the beampattern is at the endfire direction, i.e., $\theta = 0°$. We assume that the signal of interest propagates at this angle. As a result, we have

$$\begin{aligned}\mathbf{y}(\omega) &= \mathbf{d}(\omega, \cos 0°)X(\omega) + \mathbf{v}(\omega)\\ &= \mathbf{d}(\omega, 1)X(\omega) + \mathbf{v}(\omega).\end{aligned} \tag{7}$$

III. ARRAY PERFORMANCE MEASURES

Before discussing the design of different directivity patterns, let us first give three important performance measures that are commonly used in the evaluation of beamformers. They are the beampattern, the white noise gain (WNG), and the directivity index.

A. Beampattern

The beampattern, also called directivity pattern, describes the sensitivity of a beamformer to a planewave impinging on the array from the direction θ. Mathematically, it is defined as

$$\begin{aligned}\mathcal{B}[\mathbf{h}(\omega), \theta] &\triangleq \mathbf{d}^H(\omega, \cos\theta)\mathbf{h}(\omega)\\ &= \sum_{m=1}^{M} H_m(\omega) e^{j(m-1)\omega\tau_0 \cos\theta}.\end{aligned} \tag{8}$$

Figure 4 plots an example of a beampattern of a uniform linear array with five microphone sensors. The beampattern consists of a total of seven beams in the range between 0° and 360°. The one with the highest amplitude (0 dB) is called mainlobe and all the others are called sidelobes. One important parameter regarding the mainlobe is the beamwidth (sometimes also called mainlobe width), which is defined as the angle region between the −3-dB points on either side of the mainlobe. The height of the sidelobes represents the gain pattern for noise and competing sources present along the directions other than the mainlobe direction. In array and beamforming design, one hopes to make the sidelobes as low as possible so that signals coming from directions other than the mainlobe direction would be attenuated as much as possible. In addition, there are a number of directions where $\mathcal{B}[\mathbf{h}(\omega), \theta] = 0$. These are called nulls of the beampattern. As we pointed out before and will be discussed again later, the information about these nulls can be used to optimize DMA beamforming filters.

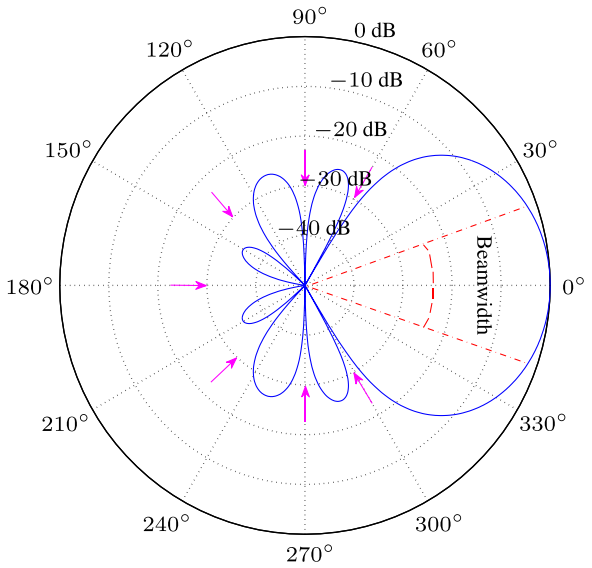

FIG. 4. (Color online) Illustration of a beampattern with a uniform linear array.

B. White noise gain

From (2) and the fact that the first microphone is the reference, we define the input signal-to-noise ratio (SNR) as

$$\mathrm{iSNR}(\omega) \triangleq \frac{\phi_X(\omega)}{\phi_{V_1}(\omega)}, \tag{9}$$

where $\phi_X(\omega) \triangleq E[|X(\omega)|^2]$ and $\phi_{V_1}(\omega) \triangleq E[|V_1(\omega)|^2]$ are the variances of $X(\omega)$ and $V_1(\omega)$, respectively, with $E[\cdot]$ denoting mathematical expectation.

According to (6), the output SNR can be written as

$$\begin{aligned}\mathrm{oSNR}[\mathbf{h}(\omega)] &\triangleq \phi_X(\omega)\frac{|\mathbf{h}^H(\omega)\mathbf{d}(\omega, \cos 0°)|^2}{\mathbf{h}^H(\omega)\mathbf{\Phi}_{\mathbf{v}}(\omega)\mathbf{h}(\omega)},\\ &= \frac{\phi_X(\omega)}{\phi_{V_1}(\omega)} \times \frac{|\mathbf{h}^H(\omega)\mathbf{d}(\omega, \cos 0°)|^2}{\mathbf{h}^H(\omega)\mathbf{\Gamma}_{\mathbf{v}}(\omega)\mathbf{h}(\omega)}\end{aligned} \tag{10}$$

where

$$\mathbf{\Phi}_{\mathbf{v}}(\omega) \triangleq E[\mathbf{v}(\omega)\mathbf{v}^H(\omega)] \tag{11}$$

and

$$\mathbf{\Gamma}_{\mathbf{v}}(\omega) \triangleq \frac{\mathbf{\Phi}_{\mathbf{v}}(\omega)}{\phi_{V_1}(\omega)} \tag{12}$$

are the correlation and pseudo-coherence matrices of $\mathbf{v}(\omega)$, respectively. From (10), we deduce that the SNR gain is

$$\mathcal{G}[\mathbf{h}(\omega)] \triangleq \frac{\mathrm{oSNR}[\mathbf{h}(\omega)]}{\mathrm{iSNR}(\omega)} = \frac{|\mathbf{h}^H(\omega)\mathbf{d}(\omega, \cos 0°)|^2}{\mathbf{h}^H(\omega)\mathbf{\Gamma}_{\mathbf{v}}(\omega)\mathbf{h}(\omega)}. \tag{13}$$

Assume that the matrix $\mathbf{\Gamma}_{\mathbf{v}}(\omega)$ is nonsingular. In this case, for any two vectors $\mathbf{h}(\omega)$ and $\mathbf{d}(\omega, \cos 0°)$, we have

$$\begin{aligned}&|\mathbf{h}^H(\omega)\mathbf{d}(\omega, \cos 0°)|^2\\ &\quad\le [\mathbf{h}^H(\omega)\mathbf{\Gamma}_{\mathbf{v}}(\omega)\mathbf{h}(\omega)]\\ &\qquad\times [\mathbf{d}^H(\omega, \cos 0°)\mathbf{\Gamma}_{\mathbf{v}}^{-1}(\omega)\mathbf{d}(\omega, \cos 0°)],\end{aligned} \tag{14}$$

where equality holds if and only if $\mathbf{h}(\omega) \propto \mathbf{\Gamma}_{\mathbf{v}}^{-1}(\omega)\,\mathbf{d}(\omega, \cos 0°)$. Using the inequality (14) in (13), we deduce an upper bound for the gain:

$$\mathcal{G}[\mathbf{h}(\omega)] \leq \mathbf{d}^H(\omega, \cos 0^\circ)\mathbf{\Gamma}_{\mathbf{v}}^{-1}(\omega)\mathbf{d}(\omega, \cos 0^\circ)$$
$$\leq \text{tr}[\mathbf{\Gamma}_{\mathbf{v}}^{-1}(\omega)]\text{tr}[\mathbf{d}(\omega, \cos 0^\circ)\mathbf{d}^H(\omega, \cos 0^\circ)]$$
$$\leq M\text{tr}[\mathbf{\Gamma}_{\mathbf{v}}^{-1}(\omega)], \quad (15)$$

where tr[·] is the trace of a square matrix. We observe how the gain is upper bounded [as long as $\mathbf{\Gamma}_{\mathbf{v}}(\omega)$ is nonsingular] and depends on the number of microphones as well as on the nature of the noise.

Now, suppose that the noise is temporally and spatially white, i.e., $\mathbf{\Gamma}_{\mathbf{v}}(\omega) = \mathbf{I}_M$, where $\mathbf{I}_M$ is the $M \times M$ identity matrix. In this case, the SNR gain is called white noise gain (WNG), i.e.,

$$\mathcal{G}_{\text{wn}}[\mathbf{h}(\omega)] = \frac{|\mathbf{h}^H(\omega)\mathbf{d}(\omega, \cos 0^\circ)|^2}{\mathbf{h}^H(\omega)\mathbf{h}(\omega)}. \quad (16)$$

In our context, the distortionless constraint is desired, i.e.,

$$\mathbf{h}^H(\omega)\mathbf{d}(\omega, \cos 0^\circ) = 1. \quad (17)$$

Then, the WNG is

$$\mathcal{G}_{\text{wn}}[\mathbf{h}(\omega)] = \frac{1}{\mathbf{h}^H(\omega)\mathbf{h}(\omega)}. \quad (18)$$

For

$$\mathbf{h}(\omega) = \frac{\mathbf{d}(\omega, \cos 0^\circ)}{M}, \quad (19)$$

we find the maximum possible gain, which is

$$\mathcal{G}_{\text{wn,max}}(\omega) = M. \quad (20)$$

In general, the WNG of an Nth-order DMA is

$$\mathcal{G}_{\text{wn},N}[\mathbf{h}(\omega)] = \frac{1}{\mathbf{h}^H(\omega)\mathbf{h}(\omega)} \leq M. \quad (21)$$

We will see how the white noise may be amplified by DMAs, i.e., $\mathcal{G}_{\text{wn},N}[\mathbf{h}(\omega)] < 1$, especially at low frequencies.

C. Directivity index

In a spherically isotropic noise field, which is often referred to as the diffuse noise field, the (i, j)th element of the noise pseudo-coherence matrix can be written as

$$[\mathbf{\Gamma}_{\mathbf{v}}(\omega)]_{ij} = [\mathbf{\Gamma}_{\text{dn}}(\omega)]_{ij} = \frac{\sin[\omega(j-i)\tau_0]}{\omega(j-i)\tau_0}$$
$$= \text{sinc}[\omega(j-i)\tau_0]. \quad (22)$$

Substituting (22) into (13), we obtain the SNR gain in diffuse noise, $\mathcal{G}_{\text{dn}}[\mathbf{h}(\omega)]$, i.e., the directivity factor. The directivity index is simply defined as (Beranek, 1986; Elko, 2000; Elko and Meyer, 2008)

$$\mathcal{D}[\mathbf{h}(\omega)] \triangleq 10\log_{10}\mathcal{G}_{\text{dn}}[\mathbf{h}(\omega)]. \quad (23)$$

In the rest, we denote by $\mathcal{G}_{\text{dn},N}[\mathbf{h}(\omega)]$ the directivity factor of an Nth-order DMA.

IV. IDEAL DMA PATTERNS

The main focus of his paper is on the design of DMA patterns. The first question that we need to answer is what is a DMA. Briefly, DMAs are a particular kind of microphone arrays that are responsive to the differential sound pressure field. Since a differential field has different orders, we also classify DMAs into different orders. Ideally, an Nth-order DMA has a pattern of the following form (Elko, 2000):

$$\mathcal{B}_N(\theta) = \sum_{n=0}^{N} a_{N,n}\cos^n\theta, \quad (24)$$

where $a_{N,n}$, $n = 0,1,\ldots, N$, are real coefficients. The different values of these coefficients give different patterns of the Nth-order DMA. In the direction of the desired signal, i.e., for $\theta = 0^\circ$, the directivity pattern must be equal to 1, i.e., $\mathcal{B}_N(0^\circ) = 1$. Therefore, we should have

$$\sum_{n=0}^{N} a_{N,n} = 1. \quad (25)$$

As a result, we always choose the first coefficient as

$$a_{N,0} = 1 - \sum_{n=1}^{N} a_{N,n}. \quad (26)$$

All interesting DMA patterns have at least one null in some direction. Since $\cos\theta$ is an even function, so is the directivity pattern $\mathcal{B}_N(\theta)$. Therefore, on a polar plot, $\mathcal{B}_N(\theta)$ is symmetric about the axis 0°–180° and any DMA design can be restricted to the range [0°, 180°]. It follows from (24) that an Nth-order DMA has at most N distinct nulls in this range.

The most popular DMAs are the first-, second-, and third-order ones.

A. First-order patterns

According to (24), the ideal pattern of the first-order DMA has the following form.

$$\mathcal{B}_1(\theta) = (1 - a_{1,1}) + a_{1,1}\cos\theta. \quad (27)$$

For the most important first-order patterns, the values of $a_{1,1}$ are as follows.

(1) Dipole: $a_{1,1} = 1$, a null at $\cos\theta = 0$, and the corresponding pattern is shown in Fig. 5(a).
(2) Cardioid: $a_{1,1} = 1/2$, a null at $\cos\theta = -1$, and the corresponding pattern is shown in Fig. 5(b).
(3) Hypercardioid: $a_{1,1} = 2/3$, a null at $\cos\theta = -1/2$, and the corresponding pattern is shown in Fig. 5(c).
(4) Supercardioid: $a_{1,1} = 2 - \sqrt{2}$, a null at $\cos\theta = -\sqrt{2}/2$, and the corresponding pattern is shown in Fig. 5(d).

B. Second-order patterns

The ideal pattern of the second-order DMA, according to (24), is described by the following equation:

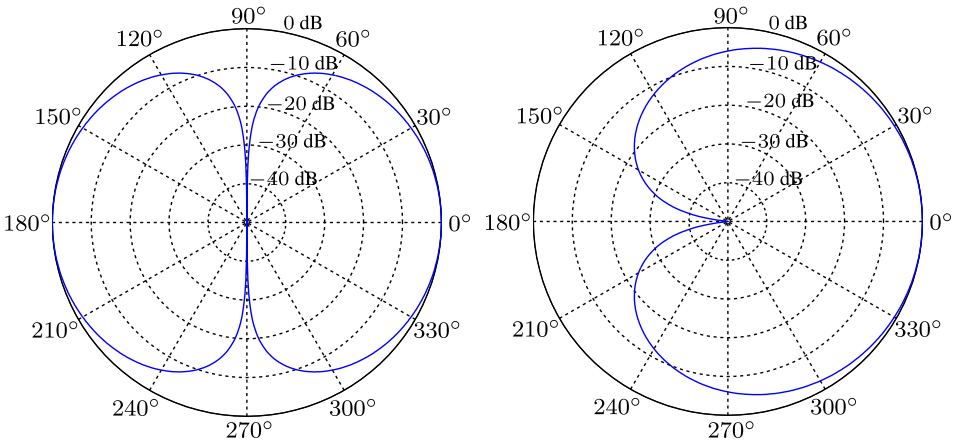

(a) Dipole (b) Cardioid

(c) Hypercardioid (d) Supercardioid

FIG. 5. (Color online) Four conventional first-order DMA patterns.

$$\mathcal{B}_2(\theta) = (1 - a_{2,1} - a_{2,2}) + a_{2,1}\cos\theta + a_{2,2}\cos^2\theta. \tag{28}$$

(1) Dipole: it has a null at $\cos\theta = 0$ and a one (maximum) at $\cos\theta = -1$. Substituting these values into (28), we find that $a_{2,1} = 0$ and $a_{2,2} = 1$. The corresponding pattern is shown in Fig. 6(a).
(2) Cardiod: it has two nulls; one at $\cos\theta = -1$ and the other at $\cos\theta = 0$. From these values, one can deduce that $a_{2,1} = a_{2,2} = 1/2$. This pattern is shown in Fig. 6(b).
(3) Hypercardioid: the Nth-order hypercardioid and supercardioid are characterized by the fact that they have N distinct nulls in the interval $0° < \theta \le 180°$. Hence, their general pattern is

$$\mathcal{B}_{\mathrm{HS},N}(\theta) = \prod_{n=1}^{N}[\varsigma_{N,n} + (1 - \varsigma_{N,n})\cos\theta], \tag{29}$$

where $\varsigma_{N,n}$, $n = 1, 2, \ldots, N$ are real coefficients. Using (28) and (29), one can find the values of $a_{2,1}$ and $a_{2,2}$ for the second-order hypercardioid, i.e., $a_{2,1} = 2/5$, $a_{2,2} = 4/5$ (Elko, 2000; Sena *et al.*, 2012). This pattern is plotted in Fig. 6(c).
(4) Supercardioid: one can also derive the values of $a_{2,1}$ and $a_{2,2}$ for the second-order supercardioid according to (28) and (29), i.e., $a_{2,1} \approx 0.484$, $a_{2,2} \approx 0.413$. This pattern is shown in Fig. 6(d) (Elko, 2000; Sena *et al.*, 2012).

C. Third-order patterns

The ideal pattern of the third-order DMA is given by

$$\mathcal{B}_3(\theta) = (1 - a_{3,1} - a_{3,2} - a_{3,3}) + a_{3,1}\cos\theta + a_{3,2}\cos^2\theta + \cos^3\theta. \tag{30}$$

The values of $a_{3,n}$ ($n = 1, 2, 3$) for four important patterns are as follows.

(1) Dipole: by analogy with the first-order and second-order dipoles, we define the Nth-order dipole as

$$\mathcal{B}_{\mathrm{D},N}(\theta) = \cos^N\theta, \tag{31}$$

implying that $a_{N,N} = 1$ and $a_{N,N-1} = a_{N,N-2} = \cdots = a_{N,0} = 0$. The Nth-order dipole has only one null (in the range 0°–180°) at $\theta = 90°$. For the third-order dipole, it can be checked that $a_{3,1} = a_{3,2} = 0$ and $a_{3,3} = 1$. The corresponding pattern is shown in Fig. 7(a).
(2) Cardioid: by analogy with the first-order and second-order cardioids, we define the Nth-order cardioid as

$$\mathcal{B}_{\mathrm{C},N}(\theta) = \left(\frac{1}{2} + \frac{1}{2}\cos\theta\right)\cos^{N-1}\theta, \tag{32}$$

implying that $a_{N,N} = a_{N,N-1} = \frac{1}{2}$ and $a_{N,N-2} = a_{N,N-3} = \cdots = a_{N,0} = 0$. This Nth-order cardioid has only two

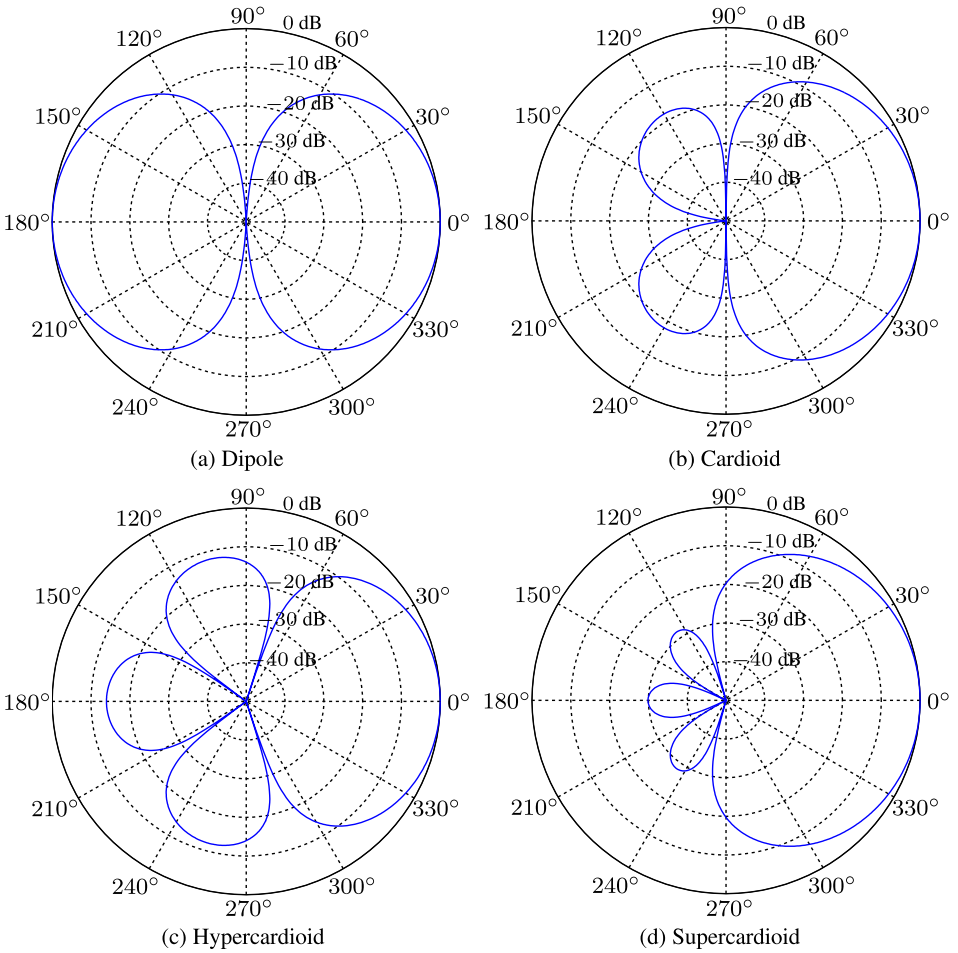

(a) Dipole (b) Cardioid

(c) Hypercardioid (d) Supercardioid

FIG. 6. (Color online) Four conventional second-order DMA patterns.

distinct nulls (in the range 0°–180°): one at $\theta = 90°$ and the other at $\theta = 180°$. So, for a third-order cardioid, we have $a_{3,1} = 0$ and $a_{3,2} = a_{3,3} = 1/2$. This pattern is plotted in Fig. 7(b).

(3) Hypercardioid: using (28) and (29), we find that $a_{3,1} = -4/7$, $a_{3,2} = 4/7$, and $a_{3,3} = 8/7$. This pattern is shown in Fig. 7(c).

(4) Supercardioid: again, with (28) and (29), we find that $a_{3,1} \approx 0.217$, $a_{3,2} \approx 0.475$, and $a_{3,3} \approx 0.286$. This pattern is shown in Fig. 7(d).

V. DESIGN OF DMA FILTERS

The objective of the DMA filter design is to find the filter coefficients in (5) so that the beampattern formed from the filter as given in (8) would approach to an ideal Nth-order DMA pattern in (24). It is seen from the previous section that an ideal DMA pattern has a one at the angle $\theta = 0°$ and a number of nulls in some specific directions. Therefore, the filter of a given linear DMA can be designed by posting one constraint at $\theta = 0°$, so that the resulting gain is equal to 1 at this direction, and a number of other constraints in the directions of the nulls. In this section, we study the filter design of an Nth-order DMA with $N+1$ microphones. We divide this general design problem into two cases: (1) the DMA has N distinct nulls and (2) the DMA has multiple nulls at the same angle.

A. Filter design with distinct nulls

Without loss of generality, we assume that the N distinct nulls are at the angles $\theta_{N,n}$, $n = 1, 2, \ldots, N$, which satisfy $0° < \theta_{N,1} < \theta_{N,2} < \cdots < \theta_{N,N} \leq 180°$. Then, we can construct the following linear system of $N+1$ equations (Benesty and Chen, 2013):

$$\mathbf{D}(\omega, \boldsymbol{\alpha})\mathbf{h}(\omega) = \mathbf{i}, \tag{33}$$

where

$$\begin{aligned}\boldsymbol{\alpha} &\triangleq [1 \;\; \alpha_{N,1} \;\; \cdots \;\; \alpha_{N,N}]^T \\ &= [\cos 0° \;\; \cos\theta_{N,1} \;\; \cdots \;\; \cos\theta_{N,N}]^T,\end{aligned} \tag{34}$$

is a vector of length $N+1$, $\alpha_{N,n} \triangleq \cos\theta_{N,n}$,

$$\mathbf{D}(\omega, \boldsymbol{\alpha}) \triangleq \begin{bmatrix} \mathbf{d}^H(\omega, 1) \\ \mathbf{d}^H(\omega, \alpha_{N,1}) \\ \vdots \\ \mathbf{d}^H(\omega, \alpha_{N,N}) \end{bmatrix} \tag{35}$$

is the constraint matrix of size $(N+1) \times (N+1)$, $\mathbf{d}(\omega, \alpha_{N,n})$ is the steering vector of length $N+1$ as defined in (4), $\mathbf{h}(\omega)$ is a filter of length $N+1$ as defined in (5),

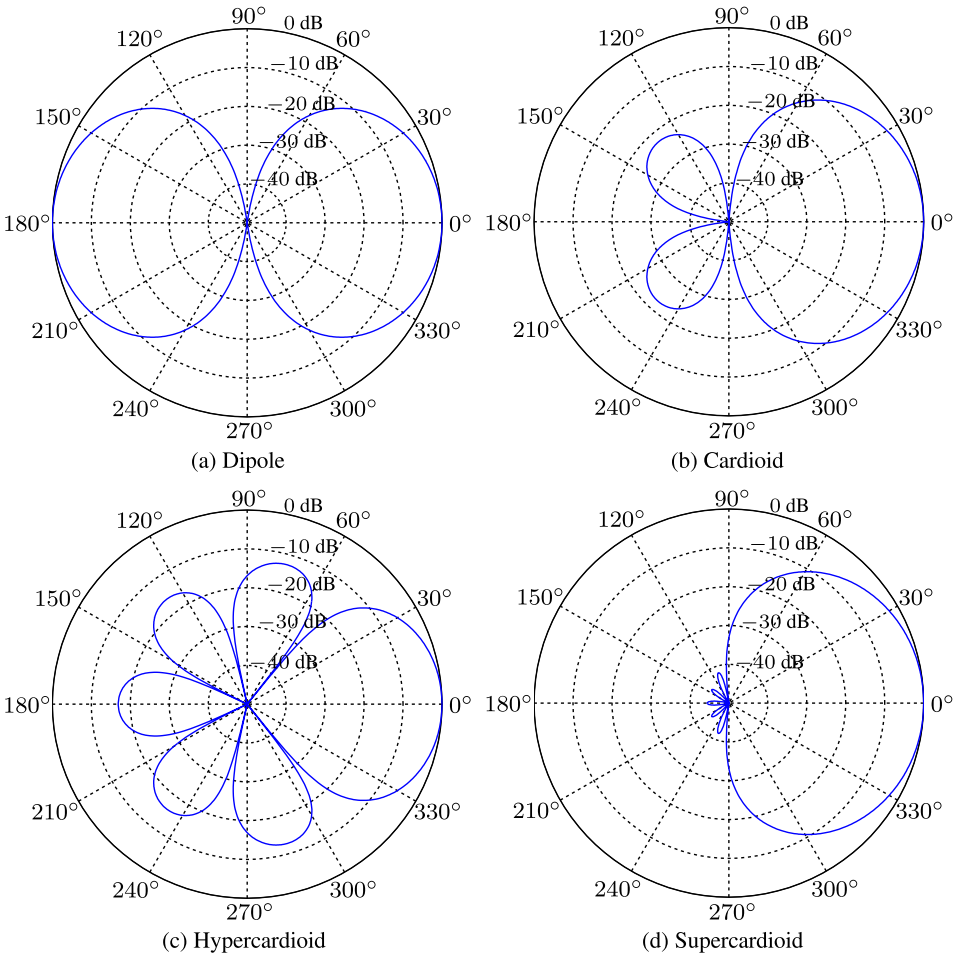

(a) Dipole (b) Cardioid

(c) Hypercardioid (d) Supercardioid

FIG. 7. (Color online) Four conventional third-order DMA patterns.

$$\mathbf{i} \triangleq [1 \ 0 \ \cdots \ 0]^T \tag{36}$$

is a vector of length $N+1$ containing the gains at the $N+1$ different angles.

Expanding all the steering vectors in (35) according to (4), we can see that $\mathbf{D}(\omega, \boldsymbol{\alpha})$ is a Vandermonde matrix of full rank (Benesty and Chen, 2013; Turner, 1966). The inverse of this matrix can be expressed as (Turner, 1966)

$$\mathbf{D}^{-1}(\omega, \boldsymbol{\alpha}) = \mathbf{U}\mathbf{L}, \tag{37}$$

where $\mathbf{U}$ and $\mathbf{L}$ are upper and lower triangular matrices of size $(N+1)\times(N+1)$, respectively. The elements l_{ij}, $i=1, 2,\ldots, N+1$, $j=1, 2,\ldots, N+1$, of $\mathbf{L}$ are given by

$$l_{ij} = \begin{cases} 0, & i < j \\ 1, & i = j = 1 \\ \displaystyle\prod_{p=1, p\neq j}^{i} \frac{1}{e^{j\omega\tau_0\alpha_{N,j-1}} - e^{j\omega\tau_0\alpha_{N,p-1}}}, & \text{otherwise}, \end{cases} \tag{38}$$

where $\alpha_{N,0} \triangleq \cos 0^\circ = 1$. The elements u_{ij}, $i=1, 2,\ldots, N+1$, $j=1, 2,\ldots, N+1$, of $\mathbf{U}$ are given by (Turner, 1966)

$$u_{ij} = \begin{cases} 1, & j = i \\ 0, & j = 1 \\ u_{i-1,j-1} - u_{i,j-1} e^{j\omega\tau_0\alpha_{N,j-2}}, & \text{otherwise}, \end{cases} \tag{39}$$

where

$$u_{0j} = 0. \tag{40}$$

Using (37), we can write the solution of (33) as

$$\mathbf{h}(\omega) = \mathbf{D}^{-1}(\omega, \boldsymbol{\alpha})\mathbf{i} = \mathbf{U}\mathbf{L}\mathbf{i}. \tag{41}$$

1. First-order patterns

For the general first-order DMA with one null, we have the following linear system of two equations:

$$\begin{bmatrix} 1 & e^{j\omega\tau_0} \\ 1 & e^{j\omega\tau_0\alpha_{1,1}} \end{bmatrix} \mathbf{h}(\omega) = \begin{bmatrix} 1 \\ 0 \end{bmatrix}. \tag{42}$$

The DMA filter is then

$$\mathbf{h}(\omega) = \frac{1}{1 - e^{j\omega\tau_0(1-\alpha_{1,1})}} \begin{bmatrix} 1 \\ -e^{-j\omega\tau_0\alpha_{1,1}} \end{bmatrix}. \tag{43}$$

Depending on how the coefficient $\alpha_{1,1}$ is chosen, we can have different patterns. For $\alpha_{1,1} = \cos\theta_{1,1} = 0$ (i.e., $\theta_{1,1} = 90^\circ$), we get the dipole; for $\alpha_{1,1} = \cos\theta_{1,1} = -1$ (i.e., $\theta_{1,1} = 180^\circ$), we get the cardioid; and for $\alpha_{1,1} = \cos\theta_{1,1} = -\sqrt{2}/2$ (i.e., $\theta_{1,1} = 135^\circ$), we obtain the supercardioid as given in Sec. IV A.

Figure 8 plots the patterns, WNGs, and directivity factors of the first-order cardioid and supercardioid designed

with (43) and $\delta = 1$ cm. It is seen that the designed patterns are the same as the ideal ones shown in Fig. 5. The cardioid has a directivity factor of approximately 5 dB and the supercardioid has a directivity factor close to 6 dB. Both the cardioid and supercardioid have a WNG smaller than 1 (or 0 dB), indicating that the DMA amplifies the white noise. This is indeed a problem with all DMAs, particularly at low frequencies. Ways to circumvent this problem are discussed in Sec. VI.

2. Second-order patterns

For the general second-order DMA and two distinct nulls, we have the following linear system of three equations:

$$\begin{bmatrix} 1 & e^{j\omega\tau_0} & e^{j2\omega\tau_0} \\ 1 & e^{j\omega\tau_0\alpha_{2,1}} & e^{j2\omega\tau_0\alpha_{2,1}} \\ 1 & e^{j\omega\tau_0\alpha_{2,2}} & e^{j2\omega\tau_0\alpha_{2,2}} \end{bmatrix} \mathbf{h}(\omega) = \begin{bmatrix} 1 \\ 0 \\ 0 \end{bmatrix}. \tag{44}$$

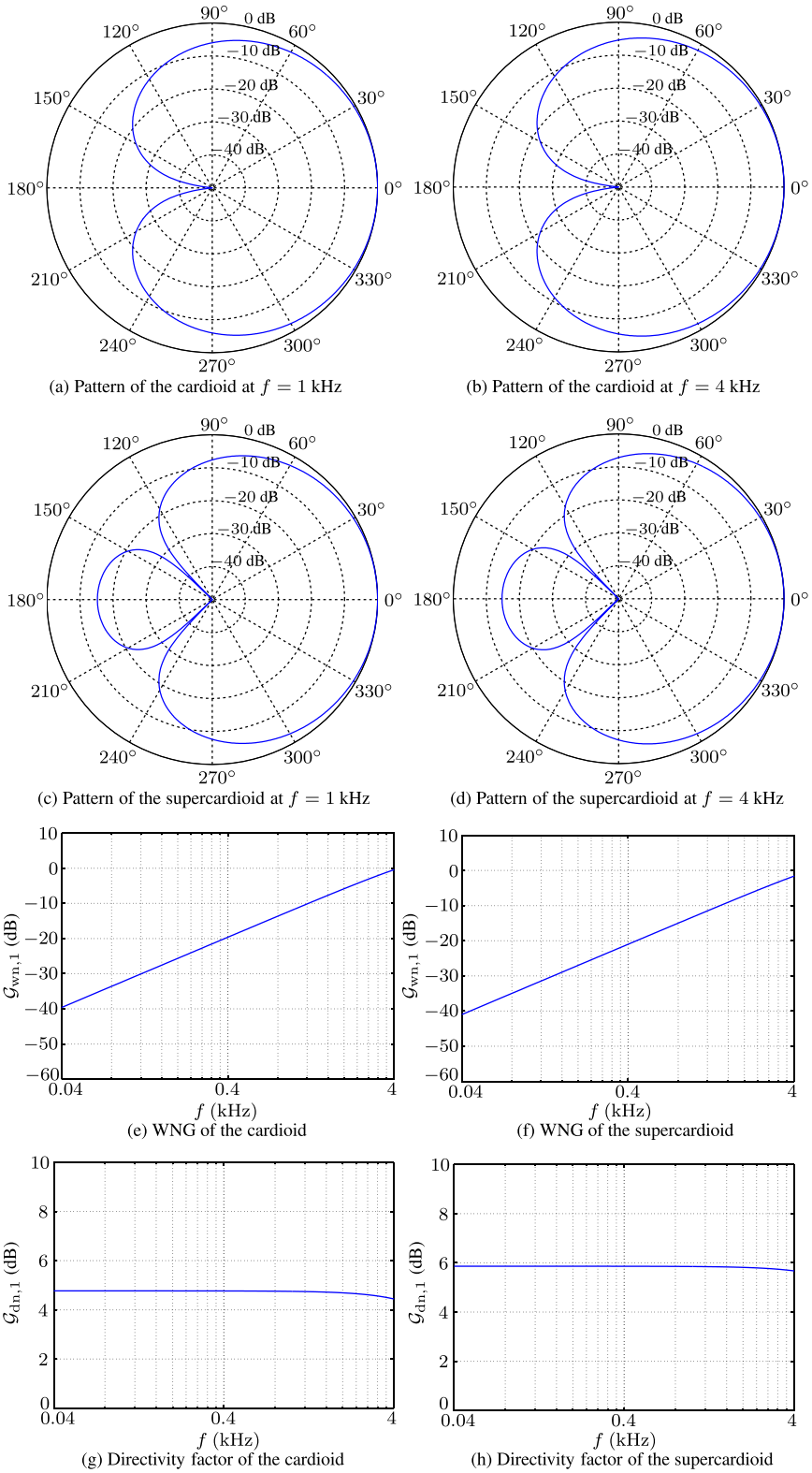

(a) Pattern of the cardioid at $f = 1$ kHz

(b) Pattern of the cardioid at $f = 4$ kHz

(c) Pattern of the supercardioid at $f = 1$ kHz

(d) Pattern of the supercardioid at $f = 4$ kHz

(e) WNG of the cardioid

(f) WNG of the supercardioid

(g) Directivity factor of the cardioid

(h) Directivity factor of the supercardioid

FIG. 8. (Color online) Patterns, WNGs, and directivity factors of the first-order cardioid and supercardioid designed with (43) and $\delta = 1$ cm.

The solution to (44) is

$$\mathbf{h}(\omega) = \frac{1}{[1 - e^{j\omega\tau_0(1-\alpha_{2,1})}][1 - e^{j\omega\tau_0(1-\alpha_{2,2})}]} \times \begin{bmatrix} 1 \\ -e^{-j\omega\tau_0\alpha_{2,1}} - e^{-j\omega\tau_0\alpha_{2,2}} \\ -e^{-j\omega\tau_0(\alpha_{2,1}+\alpha_{2,2})} \end{bmatrix}. \quad (45)$$

The values of $\alpha_{2,1}$ and $\alpha_{2,2}$ for some important patterns are as follows.

(1) Cardioid: $\alpha_{2,1} = 0$, $\alpha_{2,2} = -1$ (i.e., $\theta_{2,1} = 90°$, $\theta_{2,2} = 180°$).
(2) Hypercardioid: $\alpha_{2,1} = 0.31$, $\alpha_{2,2} = -0.81$ (i.e., $\theta_{2,1} \approx 72°$, $\theta_{2,2} \approx 144°$).
(3) Supercardioid: $\alpha_{2,1} = -0.28$, $\alpha_{2,2} = -0.89$ (i.e., $\theta_{2,1} \approx 106°$, $\theta_{2,2} \approx 153°$).

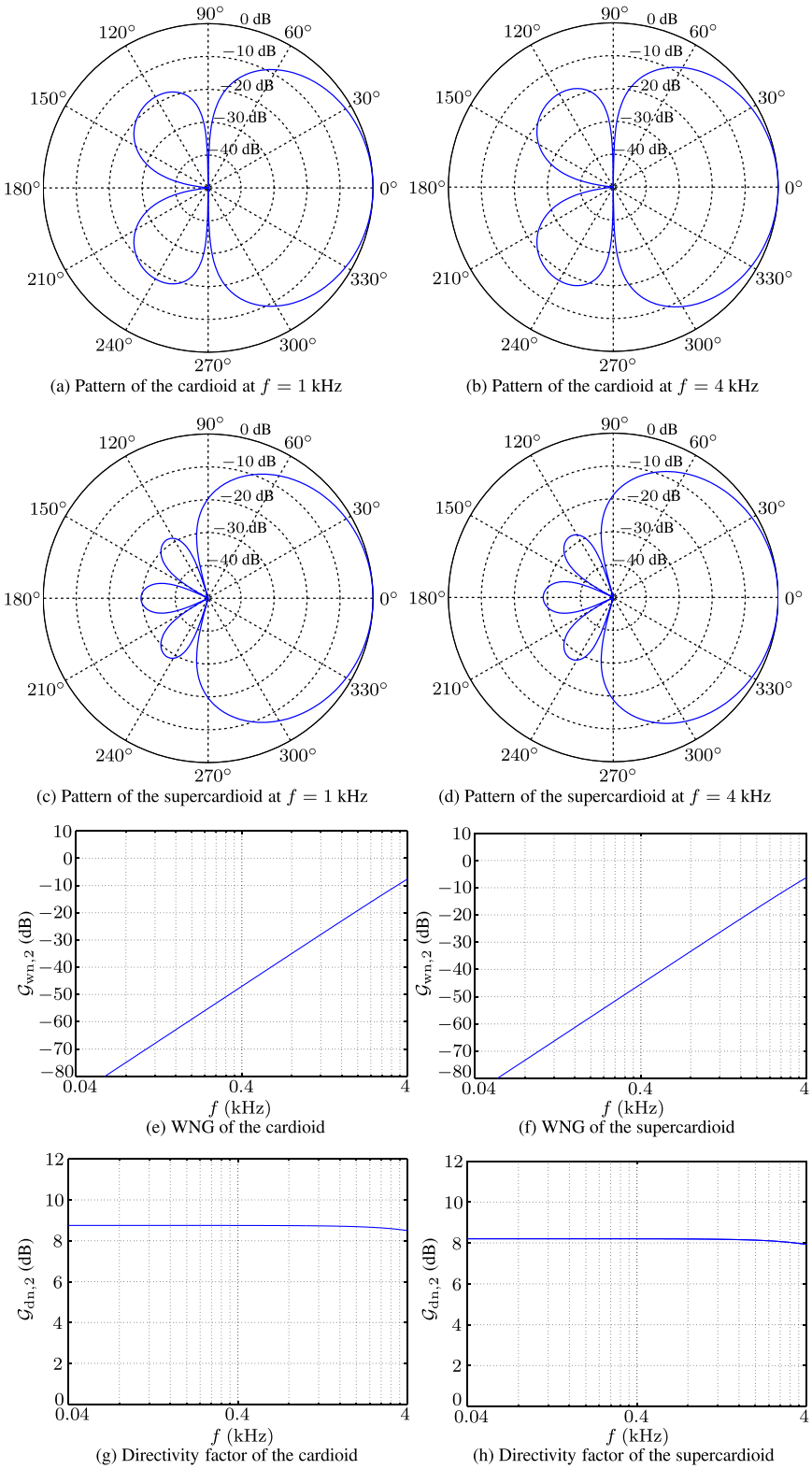

(a) Pattern of the cardioid at $f = 1$ kHz
(b) Pattern of the cardioid at $f = 4$ kHz
(c) Pattern of the supercardioid at $f = 1$ kHz
(d) Pattern of the supercardioid at $f = 4$ kHz
(e) WNG of the cardioid
(f) WNG of the supercardioid
(g) Directivity factor of the cardioid
(h) Directivity factor of the supercardioid

FIG. 9. (Color online) Patterns, WNGs, and directivity factors of the second-order cardioid and supercardioid designed with (45) and $\delta = 1$ cm.

(4) Quadrupole: $\alpha_{2,1}=\sqrt{2}/2$, $\alpha_{2,2}=-\sqrt{2}/2$ (i.e., $\theta_{2,1}=45^\circ$, $\theta_{2,2}=135^\circ$).

Figure 9 plots the patterns, WNGs, and directivity factors of the second-order cardioid and supercardioid designed with (45) and $\delta=1$ cm. Comparing this figure with Fig. 8, one can see that the beamwidth of the second-order patterns is narrower than that of the first-order patterns, and the second-order DMA can achieve a higher directivity factor than the first-order DMA, by paying the price of more white noise amplification.

3. Third-order patterns

For the general third-order DMA with three distinct nulls, we have the following linear system of three equations:

$$\begin{bmatrix} \mathbf{d}^H(\omega,1) \\ \mathbf{d}^H(\omega,\alpha_{3,1}) \\ \mathbf{d}^H(\omega,\alpha_{3,2}) \\ \mathbf{d}^H(\omega,\alpha_{3,3}) \end{bmatrix} \mathbf{h}(\omega) = \begin{bmatrix} 1 \\ 0 \\ 0 \\ 0 \end{bmatrix}, \tag{46}$$

for which the solution is

$$\mathbf{h}(\omega) = \frac{1}{[1-e^{j\omega\tau_0(1-\alpha_{3,1})}][1-e^{j\omega\tau_0(1-\alpha_{3,2})}]} \times \frac{1}{[1-e^{j\omega\tau_0(1-\alpha_{3,3})}]} \begin{bmatrix} 1 \\ \gamma_1 \\ \gamma_2 \\ \gamma_3 \end{bmatrix}, \tag{47}$$

where

$$\gamma_1 = -e^{-j\omega\tau_0\alpha_{3,1}} - e^{-j\omega\tau_0\alpha_{3,2}} - e^{-j\omega\tau_0\alpha_{3,3}}, \tag{48}$$

$$\gamma_2 = e^{-j\omega\tau_0(\alpha_{3,1}+\alpha_{3,2})} + e^{-j\omega\tau_0(\alpha_{3,2}+\alpha_{3,3})} + e^{-j\omega\tau_0(\alpha_{3,1}+\alpha_{3,3})}, \tag{49}$$

$$\gamma_3 = e^{-j\omega\tau_0(\alpha_{3,1}+\alpha_{3,2}+\alpha_{3,3})}. \tag{50}$$

Choosing $\alpha_{3,1}=0$, $\alpha_{3,2}=-1/2$, and $\alpha_{3,3}=-1$ (i.e., $\theta_{3,1}=90^\circ$, $\theta_{3,2}=120^\circ$, and $\theta_{3,3}=180^\circ$), we obtain the supercardioid.

Figure 10 plots the patterns, WNG, and directivity factor of the third-order supercardioid designed with (47) and $\delta=1$ cm. It is seen that the third-order supercardioid has a higher directivity factor than both the first- and second-order supercardiods, but it also has a more serious problem of white noise amplification.

B. Filter design with nulls of multiplicity more than one

In this part, we consider designing an Nth-order DMA pattern that has N nulls but one of multiplicity P ($1\le P\le N$) at $\alpha_{N,n}=\cos\theta_{N,n}$. In this case, the ideal DMA pattern can be expressed as

$$\mathcal{B}_N(\theta) = \mathcal{B}_{N-P}(\theta)\times(\cos\theta-\alpha_{N,n})^P. \tag{51}$$

If we take the pth-order partial derivative of $\mathcal{B}_N(\theta)$ with respect to $\alpha=\cos\theta$, it follows immediately that

$$\frac{\partial^p \mathcal{B}_N(\theta)}{\partial\alpha^p}\bigg|_{\alpha=\alpha_{N,n}} = 0,\ p=1,2,\ldots,P-1. \tag{52}$$

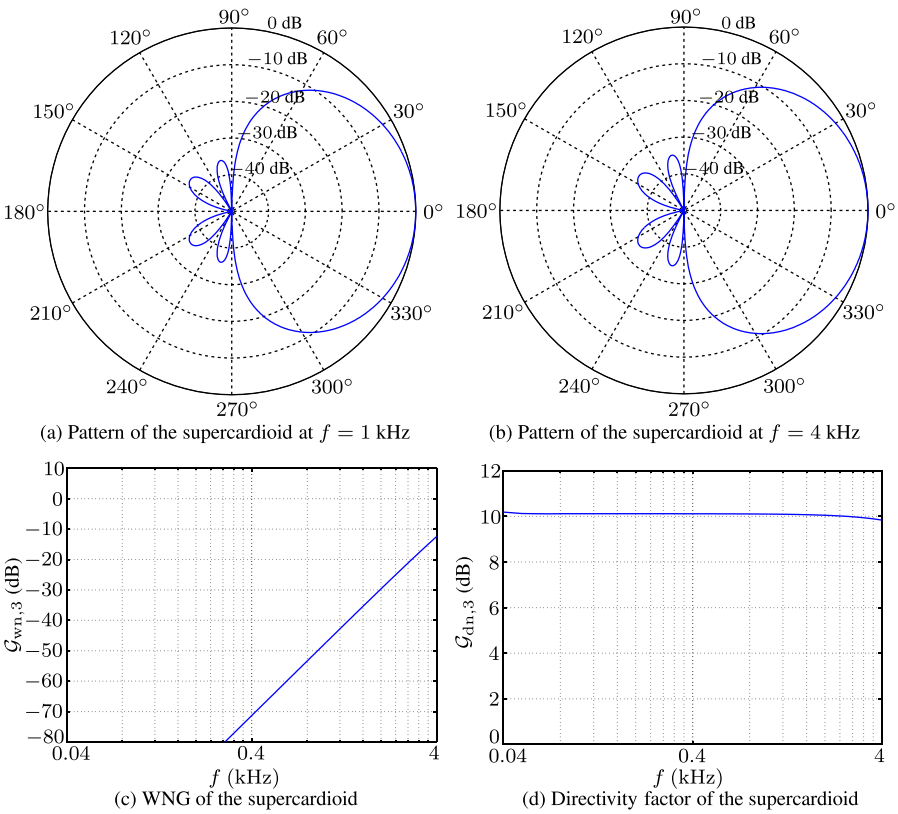

(a) Pattern of the supercardioid at $f=1$ kHz

(b) Pattern of the supercardioid at $f=4$ kHz

(c) WNG of the supercardioid

(d) Directivity factor of the supercardioid

FIG. 10. (Color online) Patterns, WNGs, and directivity factors of the third-order supercardioid designed with (47) and $\delta=1$ cm.

Now, from (8), we can derive the pth-order partial derivative of the beampattern $\mathcal{B}[\mathbf{h}(\omega),\theta]$ with respect to $\alpha=\cos\theta$ as

$$\frac{\partial^p \mathcal{B}[\mathbf{h}(\omega),\theta]}{\partial \alpha^p}=\frac{\partial^p\left[\mathbf{d}^H(\omega,\alpha)\mathbf{h}(\omega)\right]}{\partial \alpha^p}=(j\omega\tau_0)^p\left[\mathbf{\Sigma}^p\mathbf{d}(\omega,\alpha)\right]^H\mathbf{h}(\omega), \tag{53}$$

where $\mathbf{\Sigma}=\text{diag}(0,\ 1,\ldots,M-1)$ is a diagonal matrix. Comparing (52) and (53), we should have, for an Nth-order DMA having a null of multiplicity P at the angle $\theta_{N,n}$:

$$\mathbf{d}^H(\omega,\alpha_{N,n})\mathbf{h}(\omega)=0, \tag{54}$$

$$[\mathbf{\Sigma}\mathbf{d}(\omega,\alpha_{N,n})]^H\mathbf{h}(\omega)=0, \tag{55}$$

$$\vdots$$

$$[\mathbf{\Sigma}^{P-1}\mathbf{d}(\omega,\alpha_{N,n})]^H\mathbf{h}(\omega)=0. \tag{56}$$

Therefore, we can construct the following linear system of $N+1$ equations for the Nth-order DMA:

$$\mathbf{D}'(\omega,\boldsymbol{\alpha})\mathbf{h}(\omega)=\mathbf{i}, \tag{57}$$

where

$$\boldsymbol{\alpha}\triangleq[1\ \alpha_{N,1}\ \cdots\ \alpha_{N,n-1}\ \alpha_{N,n}\ \cdots\ \alpha_{N,n}\ \alpha_{N,n+P}\ \cdots\ \alpha_{N,N}]^T \tag{58}$$

is a vector of length $N+1$,

$$\mathbf{D}'(\omega,\boldsymbol{\alpha})\triangleq\begin{bmatrix}\mathbf{d}^H(\omega,1)\\ \mathbf{d}^H(\omega,\alpha_{N,1})\\ \vdots\\ \mathbf{d}^H(\omega,\alpha_{N,n})\\ \mathbf{d}^H(\omega,\alpha_{N,n})\mathbf{\Sigma}\\ \vdots\\ \mathbf{d}^H(\omega,\alpha_{N,n})\mathbf{\Sigma}^{P-1}\\ \mathbf{d}^H(\omega,\alpha_{N,n+P})\\ \vdots\\ \mathbf{d}^H(\omega,\alpha_{N,N})\end{bmatrix} \tag{59}$$

is the constraint matrix of size $(N+1)\times(N+1)$, and $\mathbf{i}$ is defined in (36). It can be checked that $\mathbf{D}'(\omega,\boldsymbol{\alpha})$ is of full rank. The solution to (57) is then

$$\mathbf{h}(\omega)=\mathbf{D}'^{-1}(\omega,\boldsymbol{\alpha})\mathbf{i}\ . \tag{60}$$

Figure 11 plots the second- and third-order cardioids designed with (60) that have a null of multiplicity 2 and 3, respectively, at 180°.

C. Filter design with ideal DMA pattern information

We discussed, in the previous subsections, how to design DMA filters using only the null position information. As long as the nulls and order of the DMA are given, the corresponding filter can be easily computed. A more general approach to the design is to include not only the null but also the directivity pattern information from other angles. Specifically, for an Nth-order DMA with $N+1$ microphones, we can form the following linear system of $N+1$ equations (Benesty and Chen, 2013):

$$\mathbf{D}(\omega,\boldsymbol{\alpha})\mathbf{h}(\omega)=\boldsymbol{\beta}, \tag{61}$$

where the constraint matrix $\mathbf{D}(\omega,\boldsymbol{\alpha})$ is defined in (35) and

$$\boldsymbol{\alpha}=[1\ \alpha_{N,1}\ \cdots\ \alpha_{N,N}]^T, \tag{62}$$

$$\boldsymbol{\beta}=[1\ \beta_{N,1}\ \cdots\ \beta_{N,N}]^T \tag{63}$$

are vectors of length $N+1$ containing the design coefficients of the directivity pattern. If $\alpha_{N,n}$ $(n=1,\ldots,N)$ corresponds to a null position, $\beta_{N,n}$ should be zero; otherwise, $\beta_{N,n}$ should be the gain at $\theta_{N,n}$ of the desired DMA pattern that we want to design. Note that the major difference between the linear system here and that in Sec. V A is that here $\alpha_{N,n}$, $n=1,\ldots,N$ may not correspond to the null positions and, therefore, this method can be used to design any DMA pattern.

However, attention has to be paid to the choice of $\alpha_{N,n}$ and $\beta_{N,n}$ to ensure that the resulting pattern is the same as the desired one. The rules of thumb are as follows.

(1) The N coefficients $\alpha_{N,n}$ should be chosen in such a way that $\mathbf{D}(\omega,\boldsymbol{\alpha})$ is well conditioned so that its inverse can be computed without any numerical problem.
(2) The N pairs of coefficients $(\alpha_{N,n},\beta_{N,n})$ should take values from the desired ideal DMA pattern.
(3) The pairs of coefficients $(\alpha_{N,n},\beta_{N,n})$ should contain all the different nulls of the desired ideal DMA pattern.

If the above rules are satisfied, The filter can be found as

$$\mathbf{h}(\omega)=\mathbf{D}^{-1}(\omega,\boldsymbol{\alpha})\boldsymbol{\beta}. \tag{64}$$

VI. WNG IMPROVEMENT

From the previous sections, one can see that a DMA may have a WNG smaller than 1, meaning that it amplifies white noise, particularly at low frequencies. The higher the DMA order, the more severe is this amplification. Indeed, this is one of the most important issues in DMAs. Ways to circumvent this fundamental problem is by using more than $N+1$ microphones to design an Nth-order DMA as discussed in the following subsections.

A. Maximization of the WNG

Suppose that we have a linear array with M $(M\geq N+1)$ microphones and we want to design an Nth-order DMA with the highest WNG. From the previous sections, we know that an Nth-order DMA can be designed by solving the linear system of $N+1$ equations, i.e.,

$$\mathbf{D}(\omega,\boldsymbol{\alpha})\mathbf{h}(\omega)=\boldsymbol{\beta}, \tag{65}$$

where $\mathbf{h}(\omega)$ is a filter of length M, but now

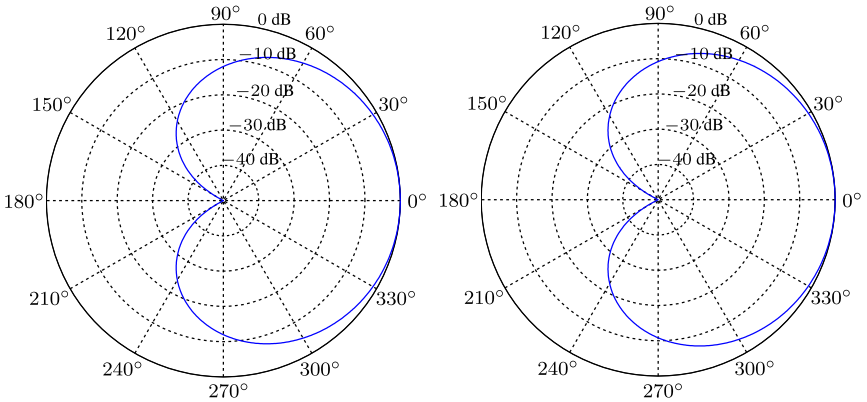

(a) Pattern of the second-order cardioid at $f = 1$ kHz

(b) Pattern of the second-order cardioid at $f = 4$ kHz

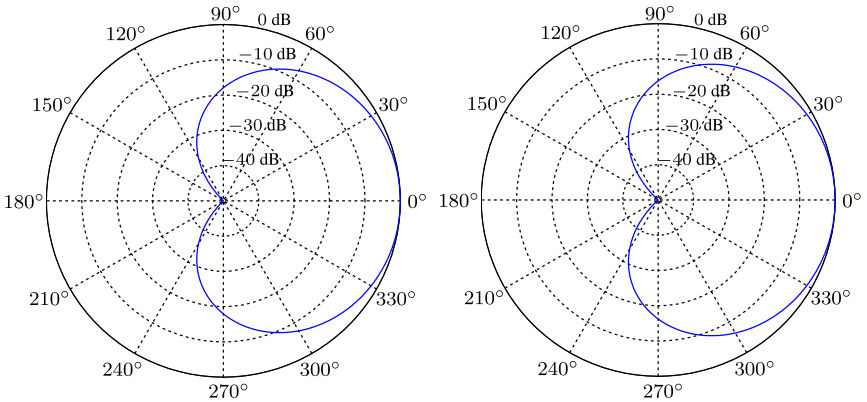

(c) Pattern of the third-order cardioid at $f = 1$ kHz

(d) Pattern of the third-order cardioid at $f = 4$ kHz

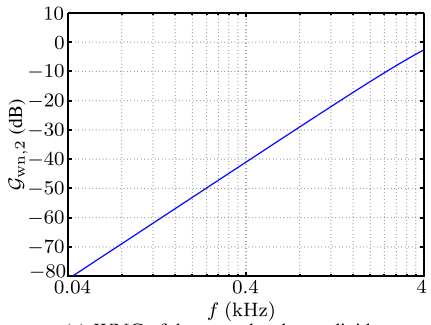

(e) WNG of the second-order cardioid

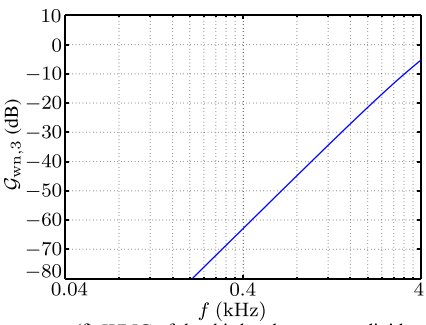

(f) WNG of the third-order supercardioid

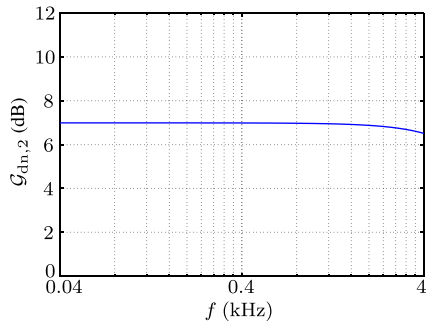

(g) Directivity factor of the second-order cardioid

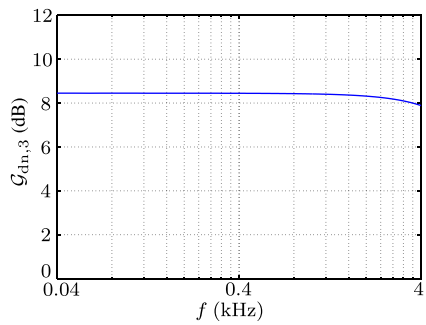

(h) Directivity factor of the third-order cardioid

FIG. 11. (Color online) Patterns, WNGs, and directivity factors of the second-order cardioid (with one null of multiplicity 2 at 180°) and third-order cardioid (with one null of multiplicity 3 at 180°) designed with (40) and $\delta = 1$ cm.

$$\mathbf{D}(\omega,\boldsymbol{\alpha}) = \begin{bmatrix} \mathbf{d}^H(\omega,1) \\ \mathbf{d}^H(\omega,\alpha_{N,1}) \\ \vdots \\ \mathbf{d}^H(\omega,\alpha_{N,N}) \end{bmatrix} \tag{66}$$

is the constraint matrix of size $(N+1)\times M$,

$$\mathbf{d}(\omega,\alpha_{N,n}) = [1 \;\; e^{-j\omega\tau_0\alpha_{N,n}} \;\; \cdots \;\; e^{-j(M-1)\omega\tau_0\alpha_{N,n}}]^T, \quad n = 1,2,\ldots,N \tag{67}$$

is the steering vector of length M, and

$$\boldsymbol{\alpha} = [1 \;\; \alpha_{N,1} \;\; \cdots \;\; \alpha_{N,N}]^T, \tag{68}$$

$$\boldsymbol{\beta} = [1 \;\; \beta_{N,1} \;\; \cdots \;\; \beta_{N,N}]^T \tag{69}$$

are vectors of length $N+1$ containing the design coefficients of the Nth-order DMA.

Now, the problem of designing an Nth-order DMA with maximum WNG can be described, according to (21), as

$$\max_{\mathbf{h}(\omega)} \frac{1}{\mathbf{h}^H(\omega)\mathbf{h}(\omega)} \quad \text{subject to} \quad \mathbf{D}(\omega,\boldsymbol{\alpha})\mathbf{h}(\omega) = \boldsymbol{\beta}, \tag{70}$$

which is equivalent to

$$\min_{\mathbf{h}(\omega)} \mathbf{h}^H(\omega)\mathbf{h}(\omega) \quad \text{subject to} \quad \mathbf{D}(\omega,\boldsymbol{\alpha})\mathbf{h}(\omega) = \boldsymbol{\beta}. \tag{71}$$

The solution of (71) leads to the maximum WNG (MaxWNG) filter

$$\mathbf{h}_{\text{MaxWNG}}(\omega) = \mathbf{D}^H(\omega,\boldsymbol{\alpha})[\mathbf{D}(\omega,\boldsymbol{\alpha})\mathbf{D}^H(\omega,\boldsymbol{\alpha})]^{-1}\boldsymbol{\beta}, \tag{72}$$

which is the minimum-norm solution of (65).

The WNG and the directivity factor of the above MaxWNG filter are, respectively,

$$\mathcal{G}_{\text{wn}}[\mathbf{h}_{\text{MaxWNG}}(\omega)] = \frac{1}{\boldsymbol{\beta}^T\left[\mathbf{D}(\omega,\boldsymbol{\alpha})\mathbf{D}^H(\omega,\boldsymbol{\alpha})\right]^{-1}\boldsymbol{\beta}} \tag{73}$$

and

$$\mathcal{G}_{\text{dn}}[\mathbf{h}_{\text{MaxWNG}}(\omega)] = \frac{1}{\mathbf{h}^H_{\text{MaxWNG}}(\omega)\boldsymbol{\Gamma}_{\text{dn}}(\omega)\mathbf{h}_{\text{MaxWNG}}(\omega)}. \tag{74}$$

It is easy to check that if $M = N+1$, the MaxWNG filter degenerates to the DMA filter designed in Sec. V. If $M > N+1$, the MaxWNG filter has the potential to form an Nth-order DMA with less white noise amplification or even a WNG greater than 1. It should be mentioned that in this case the array length is larger as compared to the case of $M = N+1$.

Figure 12 plots the patterns and WNGs of the first-order cardioid (given in Sec. V A 1) designed according to (72) with 2, 5, 10, and 30 microphones. It is clearly seen that the WNG increases with the number of microphones. With 30 microphones, there is approximately 15 dB SNR gain for most of the frequencies.

Note that if M is much larger than $N+1$, the order of the DMA may not be equal to N anymore as seen in Fig. 12. As a result, the resulting shape of the beampattern may be slightly different from the one obtained with $M = N+1$. This approach is optimal as long as the WNG is concerned. However, one can still design the ideal Nth-order DMA pattern with M microphones by adding more constraints, which is discussed in the next subsection.

B. Minimum-norm approach with additional constraints

If M is much larger than $N+1$, we can design an Nth-order DMA using more constraints than the $N+1$ fundamental constraints. Now, suppose that we have K more constraints at $(\underline{\alpha}_{K,k}, \underline{\beta}_{K,k})$, $k = 1, 2, \ldots, K$, where $\underline{\alpha}_{K,k}$'s $(-1 < \underline{\alpha}_{K,k} < 1)$ are different from all the $\alpha_{N,n}$'s. The linear system can then be constructed as

$$\tilde{\mathbf{D}}(\omega,\tilde{\boldsymbol{\alpha}})\mathbf{h}(\omega) = \tilde{\boldsymbol{\beta}}, \tag{75}$$

where

$$\tilde{\mathbf{D}}(\omega,\tilde{\boldsymbol{\alpha}}) = \begin{bmatrix} \mathbf{D}(\omega,\boldsymbol{\alpha}) \\ \underline{\mathbf{D}}(\omega,\underline{\boldsymbol{\alpha}}) \end{bmatrix}, \tag{76}$$

$$\tilde{\boldsymbol{\beta}} = \begin{bmatrix} \boldsymbol{\beta} \\ \underline{\boldsymbol{\beta}} \end{bmatrix}, \tag{77}$$

the matrix $\mathbf{D}(\omega, \boldsymbol{\alpha})$ and vector $\boldsymbol{\beta}$ are defined in (66) and (69) [note that $\mathbf{D}'(\omega, \boldsymbol{\alpha})$ defined in (59) can be used instead],

$$\underline{\boldsymbol{\alpha}} = [\underline{\alpha}_{K,1} \; \underline{\alpha}_{K,2} \; \cdots \; \underline{\alpha}_{K,K}]^T, \tag{78}$$

$$\underline{\mathbf{D}}(\omega,\underline{\boldsymbol{\alpha}}) = \begin{bmatrix} \mathbf{d}^H(\omega,\underline{\alpha}_{K,1}) \\ \mathbf{d}^H(\omega,\underline{\alpha}_{K,2}) \\ \vdots \\ \mathbf{d}^H(\omega,\underline{\alpha}_{K,K}) \end{bmatrix}, \tag{79}$$

and

$$\underline{\boldsymbol{\beta}} = [\underline{\beta}_{K,1} \; \underline{\beta}_{K,2} \; \cdots \; \underline{\beta}_{K,K}]^T. \tag{80}$$

Now, similar to the previous section, we can design an Nth-order DMA by solving the following problem:

$$\min_{\mathbf{h}(\omega)} \mathbf{h}^H(\omega)\mathbf{h}(\omega) \quad \text{subject to} \quad \tilde{\mathbf{D}}(\omega,\tilde{\boldsymbol{\alpha}})\mathbf{h}(\omega) = \tilde{\boldsymbol{\beta}}. \tag{81}$$

The solution of (81) gives another maximum WNG (MaxWNG) filter

$$\mathbf{h}'_{\text{MaxWNG}}(\omega) = \tilde{\mathbf{D}}^H(\omega,\tilde{\boldsymbol{\alpha}})[\tilde{\mathbf{D}}(\omega,\tilde{\boldsymbol{\alpha}})\tilde{\mathbf{D}}^H(\omega,\tilde{\boldsymbol{\alpha}})]^{-1}\tilde{\boldsymbol{\beta}}, \tag{82}$$

which is the minimum-norm solution of (75). The corresponding WNG is

$$\mathcal{G}_{\text{wn}}\left[\mathbf{h}'_{\text{MaxWNG}}(\omega)\right] = \frac{1}{\tilde{\boldsymbol{\beta}}^T\left[\tilde{\mathbf{D}}(\omega,\tilde{\boldsymbol{\alpha}})\tilde{\mathbf{D}}^H(\omega,\tilde{\boldsymbol{\alpha}})\right]^{-1}\tilde{\boldsymbol{\beta}}}. \tag{83}$$

Figure 13 plots the patterns and WNGs of the first-order cardioid (given in Sec. V A 1) designed according to (82) with $M = 30$ and with the following:

(1) no additional constraint, in which case the $\mathbf{h}'_{\text{MaxWNG}}(\omega)$ filter degenerates to the $\mathbf{h}_{\text{MaxWNG}}(\omega)$ filter;
(2) one additional constraint at $\underline{\alpha}_{1,1} = \cos 90^\circ = 0$;
(3) three additional constraints at $\underline{\alpha}_{3,1} = \cos 45^\circ = \sqrt{2}/2$, $\underline{\alpha}_{3,2} = \cos 90^\circ = 0$, and $\underline{\alpha}_{3,3} = \cos 135^\circ = -\sqrt{2}/2$; and
(4) five additional constraints at $\underline{\alpha}_{5,1} = \cos 30^\circ = \sqrt{3}/2$, $\underline{\alpha}_{5,2} = \cos 60^\circ = 1/2$, $\underline{\alpha}_{5,3} = \cos 90^\circ = 0$, $\underline{\alpha}_{5,4} = \cos 120^\circ = -1/2$, and $\underline{\alpha}_{5,5} = \cos 150^\circ = -\sqrt{3}/2$.

It is seen that by increasing the number of constraints, the designed pattern is closer to the ideal first-order cardioid and the resulting DMA suffers more from white noise amplification. Generally, if we use M microphones to design an Nth-order DMA, we can use a minimum of $N+1$

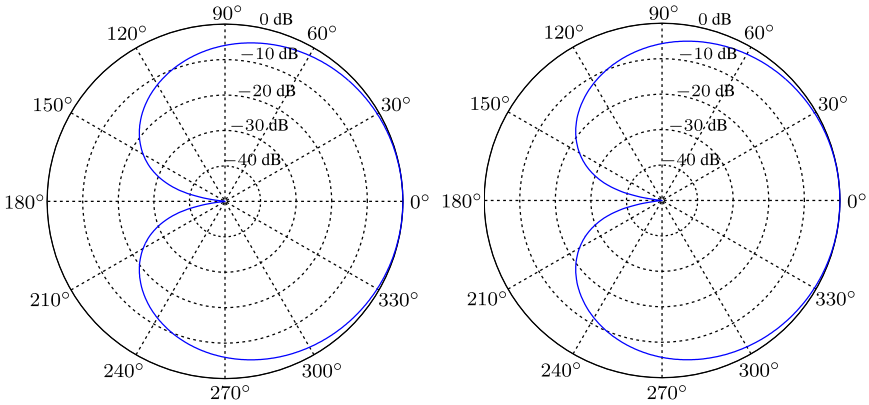

(a) Pattern of the first-order cardioid with $M = 2$

(b) Pattern of the first-order cardioid $M = 5$

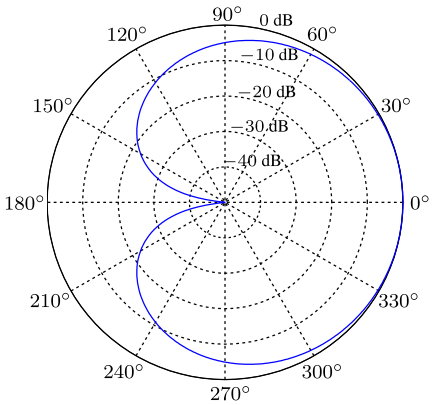

(c) Pattern of the first-order cardioid with $M = 10$

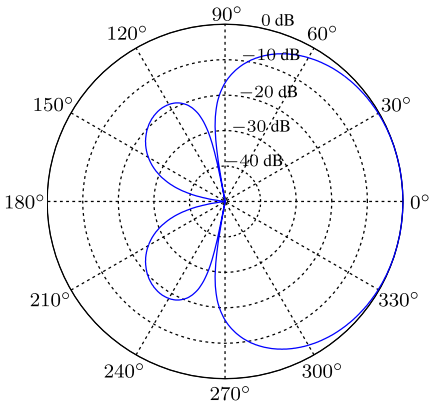

(d) Pattern of the first-order cardioid with $M = 30$

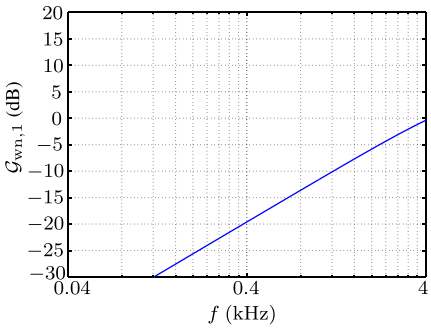

(e) WNG of the first-order cardioid with $M = 2$

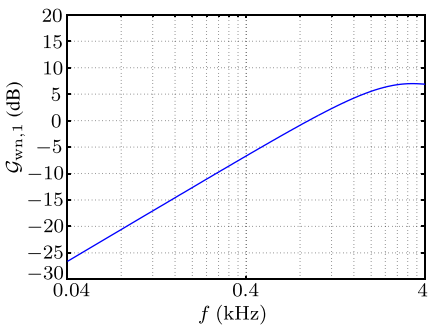

(f) WNG of the first-order cardioid with $M = 5$

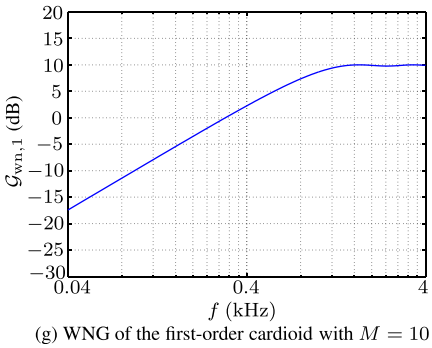

(g) WNG of the first-order cardioid with $M = 10$

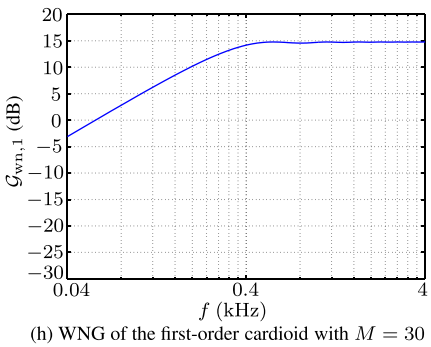

(h) WNG of the first-order cardioid with $M = 30$

FIG. 12. (Color online) Patterns (at $f = 1$ kHz) and WNGs of the first-order cardioid designed with (72), different values of M, and $\delta = 1$ cm.

constraints (the fundamental ones) and a maximum of M constraints. The more the constraints, the closer the designed pattern is to the ideal one; but there will be more white noise amplification. So, the $\mathbf{h}'_{\mathrm{MaxWNG}}(\omega)$ filter is indeed a tradeoff filter that can make a compromise between white noise amplification and ideal DMA pattern approximation.

Before finishing this section, we want to point out that careful attention has to be paid when choosing the additional constraints, just as we did for the fundamental ones. The fundamental constraints are chosen based on the DMA's null positions. The additional constraints are different from the null positions. However, they should be chosen in such a way that $\tilde{\mathbf{D}}^H(\omega, \tilde{\boldsymbol{\alpha}})$ is of full row rank.

VII. LEAST-SQUARES APPROACH

We have discussed in Sec. V the design of an Nth-order DMA using $N+1$ microphones. We also discussed in Sec. VI how to design an Nth-order DMA using more than $N+1$ microphones, which turned out to be the minimum-norm solution of a linear system with a given number of constraints. The advantage of using more microphones is that the WNG increases significantly with the number of microphones. For completeness, we briefly discuss in this section the

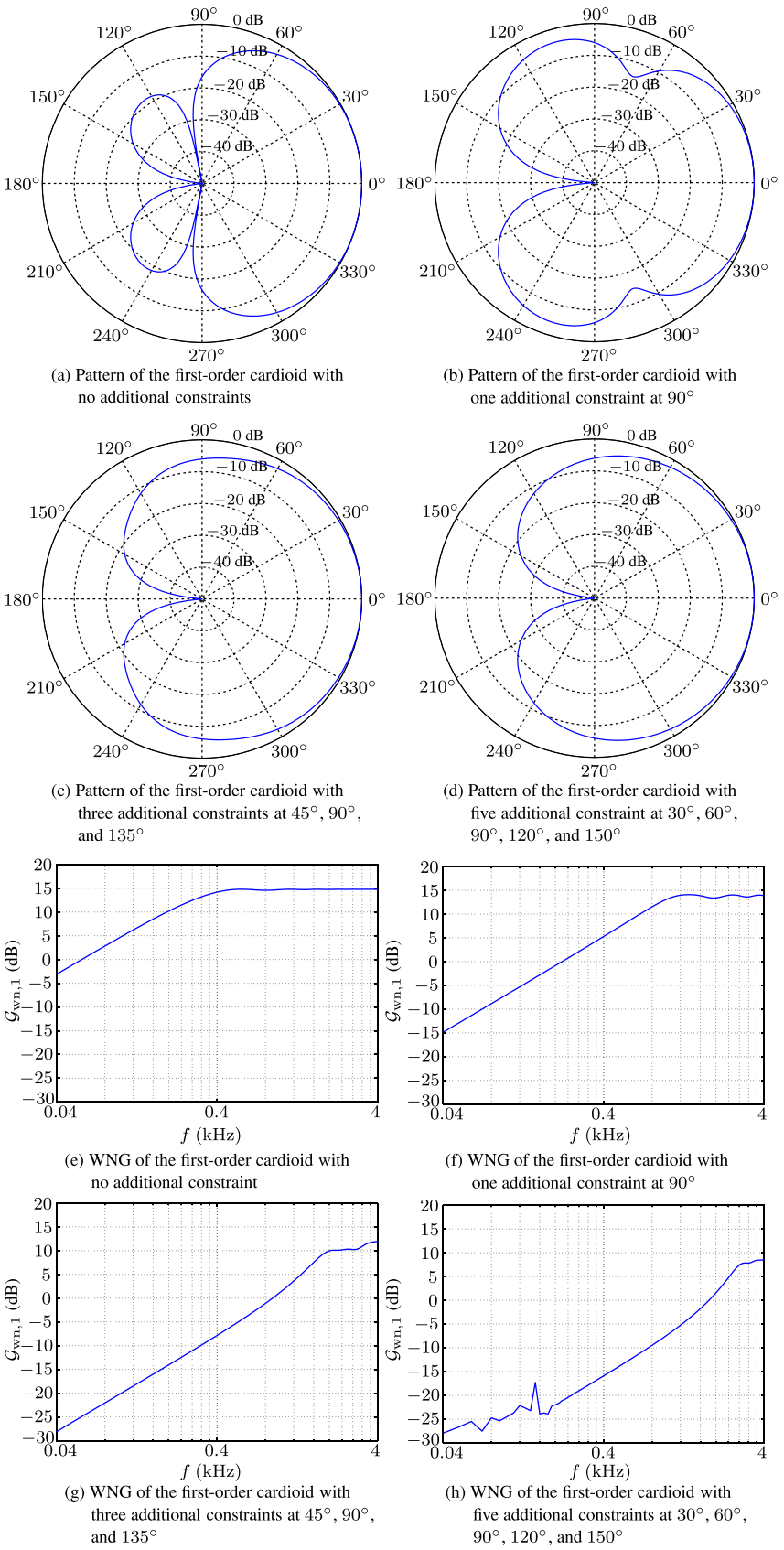

(a) Pattern of the first-order cardioid with no additional constraints

(b) Pattern of the first-order cardioid with one additional constraint at 90°

(c) Pattern of the first-order cardioid with three additional constraints at 45°, 90°, and 135°

(d) Pattern of the first-order cardioid with five additional constraint at 30°, 60°, 90°, 120°, and 150°

(e) WNG of the first-order cardioid with no additional constraint

(f) WNG of the first-order cardioid with one additional constraint at 90°

(g) WNG of the first-order cardioid with three additional constraints at 45°, 90°, and 135°

(h) WNG of the first-order cardioid with five additional constraints at 30°, 60°, 90°, 120°, and 150°

FIG. 13. (Color online) Pattern (at $f = 1$ kHz) and WNGs of the first-order cardioid designed with (82), 30 microphones, and $\delta = 1$ cm.

possibility of designing an Nth-order DMA with less than $N+1$ microphones.

Again, we assume that we have M microphones with $M<N+1$. If we want to design an Nth-order DMA, we can construct the following linear system:

$$\mathbf{D}(\omega,\boldsymbol{\alpha})\mathbf{h}(\omega)=\boldsymbol{\beta}, \tag{84}$$

where $\mathbf{h}(\omega)$ is a filter of length M as defined in Sec. II, $\mathbf{D}(\omega,\boldsymbol{\alpha})$ is the constraint matrix of size $(N+1)\times M$ similar to that defined in (66) except that now we have $M<N+1$.

Given the linear system in (84), one can find the least-squares filter

$$\mathbf{h}_{\mathrm{LS}}(\omega)=[\mathbf{D}^H(\omega,\boldsymbol{\alpha})\mathbf{D}(\omega,\boldsymbol{\alpha})]^{-1}\mathbf{D}^H(\omega,\boldsymbol{\alpha})\boldsymbol{\beta}. \tag{85}$$

Note that the fundamental constraints of an N-order DMA on the nulls may not be fulfilled with the filter given in (85) since only $M-1$ nulls can be generated given M microphones. As a result, the designed DMA may differ significantly from the ideal Nth-order DMA depending on N and M. But this is the best we can achieve given the situation.

VIII. SUMMARY

In this paper, we developed a general theory for the design and implementation of linear DMAs, which can process broadband signals such as speech. This approach works in the STFT domain. It first transforms the microphone array signals into the STFT domain. In each STFT subband, a differential beamformer is designed and applied to the multichannel noisy spectra, thereby producing an estimate of the desired signal spectrum in this subband. Finally, the time-domain desired speech estimate is constructed using the inverse STFT. Within this framework, the core issue of DMA processing is the design of the desired differential beamformer in every subband. To accomplish this, the DMA design issue is divided into three cases depending on the order of the DMA and the number of microphones. The first case covers the situation of designing an Nth-order DMA with $N+1$ microphones. Three methods were presented for this scenario, which share the common principle of converting the DMA beamforming issue into one of solving simple linear systems. The first method uses only the null information with the assumption that all the nulls are at different positions, the second one also uses only the null information but there can be multiple nulls at the same angle, whereas the third approach handles both the null information and some constraints at directions other than nulls. The second case covers the situation where an Nth-order DMA is designed using more than $N+1$ microphones. We presented two minimum-norm solutions that can approximate an Nth-order DMA by maximizing the array WNG with a given number of constraints. The last case covers the least-squares technique for the design of an Nth-order DMA with less than $N+1$ microphones.

ACKNOWLEDGMENTS

This work is supported in part by the Chinese Specialized Research Fund for the Doctoral Program of Higher Education (#: 20136102110010).

Abhayapala, T. D., and Gupta, A. (**2010**). "Higher order differential-integral microphone arrays," J. Acoust. Soc. Am. **127**, 227–233.

Benesty, J., and Chen, J. (**2013**). *Study and Design of Differential Microphone Arrays* (Springer-Verlag, Berlin, Germany), 182 pp.

Benesty, J., Chen, J., and Huang, Y. (**2008**). *Microphone Array Signal Processing* (Springer-Verlag, Berlin, Germany), 232 pp.

Benesty, J., Chen, J., Huang, Y., and Cohen, I. (**2009**). *Noise Reduction in Speech Processing* (Springer-Verlag, Berlin, Germany), 230 pp.

Beranek, L. L. (**1986**). *Acoustics* (Acoustic Society of America, Woodbury, NY), 491 pp.

Brandstein, M., and Ward, D. B. (**2001**). *Microphone Arrays: Signal Processing Techniques and Applications* (Springer-Verlag, Berlin, Germany), 398 pp.

Buck, M. (**2002**). "Aspects of first-order differential microphone arrays in the presence of sensor imperfections," Eur. Trans. Telecommun. **13**, 115–122.

Elko, G. W. (**2000**). "Superdirectional microphone arrays," in *Acoustic Signal Processing for Telecommunication*, edited by S. L. Gay and J. Benesty (Kluwer Academic Publishers, Boston, MA), Chap. 10, pp. 181–237.

Elko, G. W., and Meyer, J. (**2008**). "Microphone arrays," in *Springer Handbook of Speech Processing*, edited by J. Benesty, M. M. Sondhi, and Y. Huang(Springer-Verlag, Berlin, Germany), Chap. 50, pp. 1021–1041.

Elko, G. W., West, J. E., and Thompson, S. (**2003**). "Differential and gradient microphone arrays," J. Acoust. Soc. Am. **114**, 2426.

Flanagan, J. L., Berkeley, D. A., Elko, G. W., West, J. E., and Sondhi, M. M. (**1991**). "Autodirective microphone systems," Acustica **73**, 58–71.

Flanagan, J. L., Johnston, J. D., Zahn, R., and Elko, G. W. (**1985**). "Computer-steered microphone arrays for sound transduction in large rooms," J. Acoust. Soc. Am. **78**, 1508–1518.

Frost, O. L., III (**1972**). "An algorithm for linearly constrained adaptive array processing," Proc. IEEE **60**, 926–935.

Huang, Y., Benesty, J., and Chen, J. (**2006**). *Acoustic MIMO Signal Processing* (Springer-Verlag, Berlin, Germany), 374 pp.

Huang, Y., Chen, J., and Benesty, J. (**2011**). "Immersive audio schemes: The evolution of multiparty teleconferencing," IEEE Sig. Process. Mag. **20**, 20–32.

Kellermann, W. (**1991**). "A self-steering digital microphone array," in *IEEE International Conference on Acoustics, Speech, and Signal Processing (IEEE ICASSP)*, Vol. 5, 3581–3584.

Kolundžija, M., Faller, C., and Vetterli, M. (**2011**). "Spatiotemporal gradient analysis of differential microphone arrays," J. Audio Eng. Soc. **59**, 20–28.

Lim, J. S. (**1979**). "Enhancement and bandwidth compression of noisy speech," Proc. IEEE **67**, 1586–1604.

Olson, H. F. (**1946**). "Gradient microphones," J. Acoust. Soc. Am. **17**, 192–198.

Sena, E. D., Hacihabiboğu, H., and Cvetković, Z. (**2012**). "On the design and implementation of higher-order differential microphones," IEEE Trans. Audio Speech Lang. Process. **20**, 162–174.

Sessler, G. M., and West, J. E. (**1971**). "Directional transducers," IEEE Trans. Audio Electroacoust. **19**, 19–23.

Turner, L. R. (**1966**). "Inverse of the vandermonde matrix with applications," NASA Tech. Note D-3547 (NASA, Washington, DC).

Ward, D. B., Williamson, R. C., and Kennedy, R. A. (**1998**). "Broadband microphone arrays for speech acquisition," Acoust. Australia **26**, 17–20.